RSC Advances

PAPER

View Article Online
View Journal | View Issue

Check for updates

Cite this: *RSC Adv.*, 2020, **10**, 9686

Metallo-supramolecular complexes from mPEG/PDPA diblock copolymers and their self-assembled strip nanosheets†

Xiaoyu Zhang, Yuyang Liu, * Xin Wang, Yinxiu Liang and Lei Yan

Received 15th January 2020
Accepted 27th February 2020

DOI: 10.1039/d0ra00431f

rsc.li/rsc-advances

Herein we designed and synthesized mPEG/PDPA copolymers containing two 4-([2,2′:6′,2″-terpyridin]-4′-yl) phenyl (Tpyp) groups at the junction point of the two blocks (mPEG(-*b*-Tpyp)$_2$-*b*-PDPA$_x$, x = 23, 33, and 44). Interestingly, after a hierarchical pattern from the coordination of mPEG(-*b*-Tpyp)$_2$-*b*-PDPA$_x$ with Ru(II) ions followed by the self-assembly in water, 2D strip nanosheets with a monomolecular layer were obtained. In contrast, mPEG(-*b*-Tpyp)$_2$-*b*-PDPA$_x$ without coordination self-assembled into spherical micelles in the similar condition. The formation of the rigid and charged ···Tpyp-Ru(II)··· chain, the brush-shaped polymer architecture and the presence of the hexafluorophosphate (PF_6^-) counterions should be responsible for the unique self-assembly behavior of the metallo-supramolecular complexes. It is expected that the hierarchical self-assembly pattern can provide a new strategy for preparation of self-assemblies with different morphologies.

Open Access Article. Published on 06 March 2020. Downloaded on 2/14/2026 9:26:38 AM.
This article is licensed under a Creative Commons Attribution-NonCommercial 3.0 Unported Licence.

1. Introduction

Amphiphilic copolymers can self-assemble into various morphologic nanoaggregates in aqueous solution.[1–8] The types of copolymers have therefore potential applications in many fields such as drug delivery[9] and microcapsules.[10] Therefore, exploration of self-assemblies with novel morphologies and functions attracts many researchers' attentions. Actual morphologies of self-assemblies of amphiphilic copolymers depend on many factors such as compositions and properties of building blocks, macromolecular architecture and self-assembly conditions. As far as architecture of a polymer is concerned, it is usually established by covalent bond linking. However, for some complicated polymer architectures, the synthesis steps are tedious. Therefore, it is interesting to explore novel morphological or functional aggregates from hierarchical supramolecular self-assembly of simple macromolecules.

The ligand–metal coordination has currently been used to construct metallo-supramolecular polymers with different molecular architectures such as linear polymers,[11–15] block[16–22] and star polymers,[23–25] dendrimers[26] and even hydrogels.[25,27] Although the binding strength of ligand–metal interaction in a range of approximately between 25% and 95% of a covalent C–C bond, the coordination bonding usually exhibits directionality and reversibility.[12,18,19] Also, the presence of ligand–metal coordination moieties may endow supramolecular polymers with interesting properties or self-assembly behaviors.[25,27,28]

Macroligand–metal coordination is an important strategy to construct metallo-supramolecular polymers.[29–32] For this method, the polymer units containing ligand moieties (macroligands) are first designed and synthesized, and the tailored units are then held together through the coordination with metal ions.[12,14–24,30] Among ligand groups, 2,2′:6′,2″-terpyridine (Tpy) moiety is widely introduced into polymer building blocks for synthesizing macroligands,[12,14–23,28–32] because it is able to form stable Tpy-M-Tpy (M, metal ion) complexes with a wide range of metal ions such as Ni(II), Fe(II), Cu(II), Co(II), Zn(II), Cd(II) and Ru(II),[29–34] making the formed metallo-supramolecular polymers have a well-defined architecture.[15–23,30] Among complex species, Tpy-Ni(II)-Tpy and Tpy-Ru(II)-Tpy types exhibit good stability in water.[14] U. S. Schubert *et al.* have investigated synthesis and coordination self-assembly of Tpy-containing polymers extensively and in-depth.[12,14–21,23,29] For example, they constructed amphiphilic copolymers such as PS$_{20}$-[Ru(II)]-PEO$_{70}$ (PS, poly(styrene); PEO, poly(ethylene oxide); subscript, degree of polymerization (DP))[17] and PS$_{32}$-*b*-P2VP$_{13}$-[Ru(II)]-PEO$_{70}$ (P2VP, poly(2-vinylpyridine)).[18] Liang and Xia *et al.* also synthesized PPG-[Cu(II)]-mPEG (PPG, poly(propylene glycol); mPEG, methoxypolyethylene glycol) by the similar molecular design.[22] The metallo-supramolecular copolymers were able to self-assemble into spherical micelles in water.

Although Tpy-containing macroligands were widely investigated, more attentions were paid on synthesizing different Typ-

Key Laboratory of Macromolecular Science and Technology of Shaanxi Province, School of Chemistry and Chemical Engineering, Northwestern Polytechnical University, Xi'an 710072, P. R. China. E-mail: liu_yyang1120@nwpu.edu.cn

† Electronic supplementary information (ESI) available: Experimental methods, ^{1}H NMR and fluorescence spectra, GPC traces, TEM images and DLS measurements. See DOI: 10.1039/d0ra00431f

This journal is © The Royal Society of Chemistry 2020

Open Access Article. Published on 06 March 2020. Downloaded on 2/14/2026 9:26:38 AM.
This article is licensed under a Creative Commons Attribution-NonCommercial 3.0 Unported Licence.

ended polymers and further constructing copolymers by metal ion coordination linkage. In our opinion, for a A-*b*-B diblock copolymer, if two Tpy ligand groups are at the junction point of A and B blocks, the Tpy-M-Tpy coordination is able to drive the AB diblock copolymer units to self-assemble to form [-Typ-A(-*b*-B)-Typ-M-]$_n$ metallo-supramolecular architecture. Thus, the AB copolymer units are made directional alignment by metal ion linkage. As a result, ⋯Tpy-M⋯ chains generate, and the A/B blocks are transformed into pendant heterochains of the new supramolecular complexes. When further self-assembly of the complexes in aqueous solution, it is possible to form aggregates with a novel morphology, differing from that of precursor A-*b*-B copolymer. However, this has not been investigated yet.

Based on the consideration above, we herein designed and synthesized novel diblock copolymers containing two Tpy groups at the junction point of the two blocks, *i.e.* mPEG(-*b*-Tpyp)$_2$-*b*-PDPA$_x$ ($M_{n,\ mPEG}$ = 4000 g mol^{-1}; PDPA, poly(2-(diisopropylamino)ethyl methacrylate); Tpyp, 4-([2,2′:6′,2″-terpyridin]-4′-yl) phenyl group). Interestingly, after a hierarchical pattern from the coordination of mPEG(-*b*-Tpyp)$_2$-*b*-PDPA$_x$ with Ru(II) ions followed by the self-assembly in water, 2D strip nanosheets with a monomolecular layer were obtained and parallel stripes of the nanosheets were observed. This suggests that the self-assembly units adopted directional array. In contrast, mPEG(-*b*-Tpyp)$_2$-*b*-PDPA$_x$ copolymers without coordination self-assembled into spherical micelles in the similar condition. To our knowledge, so far this type of diblock copolymers, and their metallo-supramolecular complexes and self-assembly of the complexes have not been reported yet.

2. Results and discussion

The synthesis route for mPEG(-*b*-Tpyp)$_2$-*b*-PDPA$_x$ is shown in Scheme 1 and the experimental methods are shown in ESI.† Herein pentaerythritol was selected as the core, because of its symmetry. It is therefore suitable for constructing AB-type diblock copolymer retaining two hydroxyl groups at the block junction point for linking two ligand groups, to further construct a brush-like metallo-supramolecular architecture with pendant heterochains. Based on this, core @(–OH)$_3$–Cl was firstly synthesized *via* the reaction of one hydroxyl group of pentaerythritol with 2-chloropropionyl chloride (CPC) (Scheme 1a). Owing to pentaerythritol exhibiting low solubility in DMF at low temperature, the addition of CPC and the followed esterification were done at 50 °C. Compared with other mono-esterification method of pentaerythritol,[35] the synthesis involved one step reaction. ^{1}H NMR data of @(–OH)$_3$–Cl (Fig. S1, ESI†) confirm that it was synthesized successfully. Then, mPEG-COOH was synthesized *via* the reaction of mPEG with succinic anhydride in the presence of 4-dimethylaminopyridine (DMAP) (Scheme 1b).[36,37] In Fig. S2 (ESI†), it could be observed clearly that the new resonances at chemical shift (δ) = 4.26 and 2.66 ppm are assigned to the protons of –CH_2–O–C(=O)– and –OC(=O)–CH_2CH_2–C(=O)O– groups, respectively, in addition to the characteristic resonances of the mPEG chain at δ = 3.66 and 3.40 ppm. This means that the succinic anhydride esterified the hydroxyl group of mPEG. Thirdly, the esterification of mPEG-COOH with @(–OH)$_3$–Cl in the presence of *N*-(3-dimethylaminopropyl)-*N*′-ethylcarbodiimide hydrochloride (EDCI)/DMAP[38] afforded mPEG(–OH)$_2$–Cl (Scheme 1c). ^{1}H NMR

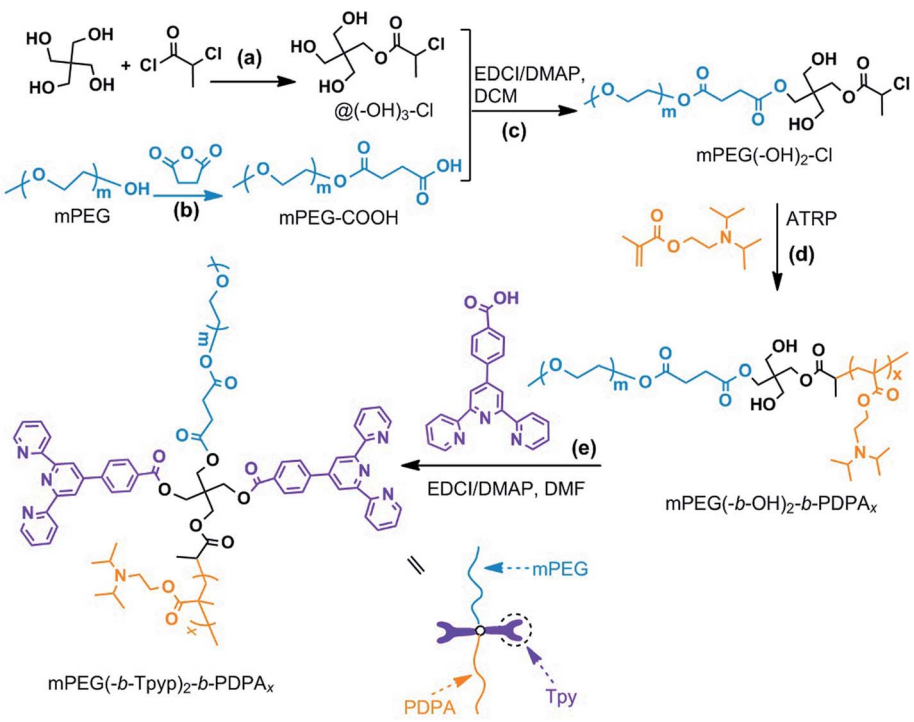

Scheme 1 Synthesis route for mPEG(-*b*-Tpyp)$_2$-*b*-PDPA$_x$, which included syntheses of (a) @(-OH)$_3$-Cl, (b) mPEG-COOH, (c) mPEG(-OH)$_2$-Cl, (d) mPEG(-*b*-OH)$_2$-*b*-PDPA$_x$ and (e) mPEG(-*b*-Tpyp)$_2$-*b*-PDPA$_x$.

Open Access Article. Published on 06 March 2020. Downloaded on 2/14/2026 9:26:38 AM.
This article is licensed under a Creative Commons Attribution-NonCommercial 3.0 Unported Licence.

Table 1 Structure data for mPEG(-*b*-OH)$_2$-*b*-PDPA$_x$ and mPEG(-*b*-Tpyp)$_2$-*b*-PDPA$_x$[a]

Synthesis of mPEG(-*b*-OH)$_2$-*b*-PDPA$_x$					mPEG(-*b*-Tpyp)$_2$-*b*-PDPA$_x$
x	mPEG(-*b*-OH)$_2$-Cl/DPA (mol mol^{-1})	$M_{n,\ NMR}$ (g mol^{-1})	$M_{n,\ GPC}$ (g mol^{-1})	M_w/M_n	x
22	1/15	8994	7084	1.15	23
31	1/20	10 911	7501	1.17	33
42	1/30	13 254	8059	1.27	44

[a] The subscript x of PDPA refers as DP of the PDPA block, which was determined by ^{1}H NMR spectrum.

spectrum of mPEG(–OH)$_2$–Cl (Fig. S3, ESI†) indicates that the resonance intensity ratio of the methoxy group of mPEG to the methyl group of the –CH(*CH*$_3$)Cl moiety is close to 1 : 1, indicating the fact that mPEG(–OH)$_2$–Cl was synthesized successfully. Fourthly, by using mPEG(–OH)$_2$–Cl as the ATRP macroinitiator, three copolymers mPEG(-*b*-OH)$_2$-*b*-PDPA$_x$ were synthesized in DMF[39] (Scheme 1d) through changing mPEG(–OH)$_2$–Cl/DPA (DPA, 2-(diisopropylamino)ethyl methacrylate) feed ratios. The structure information of mPEG(-*b*-OH)$_2$-*b*-PDPA$_x$ characterized by GPC (Fig. S4, ESI†) and ^{1}H NMR (Fig. S5, ESI†) measurements is shown in Table 1. As seen from Table 1, the molecular weight distributions (M_w/M_n) of the three mPEG(-*b*-OH)$_2$-*b*-PDPA$_x$ samples are narrow. In Fig. S5 (ESI†), the resonances at δ = 3.85, 3.01 and 2.65 ppm are assigned to the protons of the –C(=O)O*CH*$_2$–, –*CH*$_2$N[CH(CH$_3$)]$_2$– and –CH$_2$N[*CH*(CH$_3$)]$_2$ groups for the DPA units, respectively. The resonances at δ = 0.92 and 1.03 ppm are also assigned to the protons of the methyl groups of the DPA units. According to the resonance strength at δ = 3.40 from the methoxy group of the mPEG block, average x values of the PDPA blocks for the three copolymers were estimated to be 22, 31 and 42, respectively (Table 1). In this paper, the x values of the PDPA blocks were from ^{1}H NMR measurement.

mPEG(-*b*-Tpyp)$_2$-*b*-PDPA$_x$ were synthesized *via* the esterification of mPEG(-*b*-OH)$_2$-*b*-PDPA$_x$ with 4-([2,2′:6′,2″-terpyridin]-4′-yl)benzoic acid in the presence of EDCI/DMAP (Scheme 1e). In ^{1}H NMR spectra of mPEG(-*b*-Tpyp)$_2$-*b*-PDPA$_x$ by using CDCl$_3$ as the solvent (Fig. S6, ESI†), the resonances at δ = 8.69 (q, u), 8.60 (t), 8.14 (w), 7.94 (s), 7.87 (v) and 7.34 (r) ppm assigned to the protons of the Tpyp groups could be observed clearly in addition to the characteristic those of the mPEG and PDPA blocks. The resonance at δ = 4.58 (peak b‴) is assigned to the new –C(=O)O*CH*$_2$– groups formed *via* the esterification. Similarly, according to the resonance strength at δ = 3.40 from the mPEG block, it is confirmed that there are two Tpyp units per mPEG(-*b*-Tpyp)$_2$-*b*-PDPA$_x$ molecule; and their x values were estimated to be 23, 33 and 44, respectively (Table 1). Compared with those of mPEG(-*b*-OH)$_2$-*b*-PDPA$_x$, a slight increase in the x values of mPEG(-*b*-Tpyp)$_2$-*b*-PDPA$_x$ should be caused by loss of some low molecular weight copolymers *via* dialysis during the purification.

mPEG(-*b*-Tpyp)$_2$-*b*-PDPA$_x$/Ru(II) complexes (MSC23, MSC33 and MSC44, Fig. 1A) were prepared in ethanol solution at 75 °C (ESI†).[12,16] The solutions of the complexes are red, while mPEG(-*b*-Tpyp)$_2$-*b*-PDPA$_x$ solution is colorless (Fig. 1B). The formation of Tpy/Ru(II) coordination complexes was investigated by ^{1}H NMR (Fig. S7, ESI†) and UV/vis spectra (Fig. 1B). Fig. S7 (ESI†) shows ^{1}H NMR spectra in aromatic region for the Tpyp groups of sample MSC33 before and after complexing with Ru(II) ions by using CD$_3$CN as the solvent. It is clear that Tpy/Ru(II) coordination led to an evident change in chemical shifts of the Tpyp protons. For example, for protons u, q and t of the Tpy group at

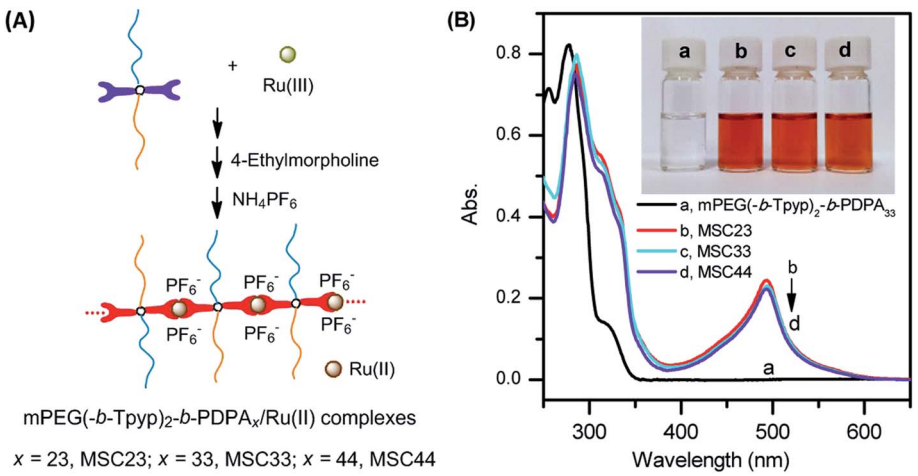

Fig. 1 Preparation route to the metallo-supramolecular complexes (A) and the UV/vis spectra of the THF solutions of the complexes (B) (sample concentration of (B), the bottles, *ca.* 1 mg mL^{-1}; UV/vis measurement, *ca.* 0.1 mg mL^{-1}).

 This journal is © The Royal Society of Chemistry 2020

Open Access Article. Published on 06 March 2020. Downloaded on 2/14/2026 9:26:38 AM.
This article is licensed under a Creative Commons Attribution-NonCommercial 3.0 Unported Licence.

$\delta = 8.54$ ppm, after the Tpy group coordinated with Ru(II) ion their chemical shifts shifted to 9.16 (u′), 7.43 (q′) and 8.76 (t′) ppm, respectively. This confirms that mPEG(-*b*-Tpyp)$_2$-*b*-PDPA$_{33}$/Ru(II) complex formed.[11,12] In Fig. 1B, the solutions of MSC23, MSC33 and MSC44 all exhibited evident characteristic metal-to-ligand charge-transfer (MLCT) absorption band of bis(terpyridine)-Ru(II) complex at 494 nm.[11,16,17] This means that the complexes formed by bis(terpyridine)-Ru(II) coordination. This suggests that multiple mPEG(-*b*-Tpyp)$_2$-*b*-PDPA$_x$ units were connected through Ru(II) ions. As a result, a rigid ···Tpyp-Ru(II)··· chain was created and the mPEG/PDPA blocks changed into the pendant heterochains of the new architecture.

Self-assembly of the metallo-supramolecular complexes was carried out through stepwise addition of water into their THF solutions. The THF was afterwards removed by reduced pressure. Interestingly, MSC23 and MSC33 mainly self-assembled into strip nanosheets (Fig. 2a1 and b1), which show several nanometers in width and tens of nanometers in length. But there were evident synechiae among the nanosheets. Under high resolution (*e.g.* the aggregates in the boxes of Fig. 2a1 and b1), the parallel stripes along the length direction of the nanosheets are observed (Fig. 2a2 and b2). This suggests that the self-assembly of MSC23 and MSC33 adopted highly directional array. The thickness of the nanosheets was determined by AMF images to be *ca.* 3.5 nm (Fig. 2a3 and b3). Note, the AMF images should also be a result of synechia of multiple strip nanosheets. Although the self-assembly of MSC44 produced spherical micelles (Fig. 2c1) besides some strip nanosheets (Fig. 2c2), the nanosheets still show parallel stripes like those of MSC23 and MSC33 self-assemblies. In Fig. 2c3, images af-3 and af-4 may correspond to sheet and spherical morphologies, respectively. These results imply that x values of the PDPA blocks affected actual self-assembled morphologies of the supramolecular complexes. In contrast, copolymers mPEG(-*b*-Tpyp)$_2$-*b*-PDPA$_x$ formed spherical micelles (Fig. S8, ESI†). Self-assembly behaviors of analogous copolymers mPEG-*b*-PDPA

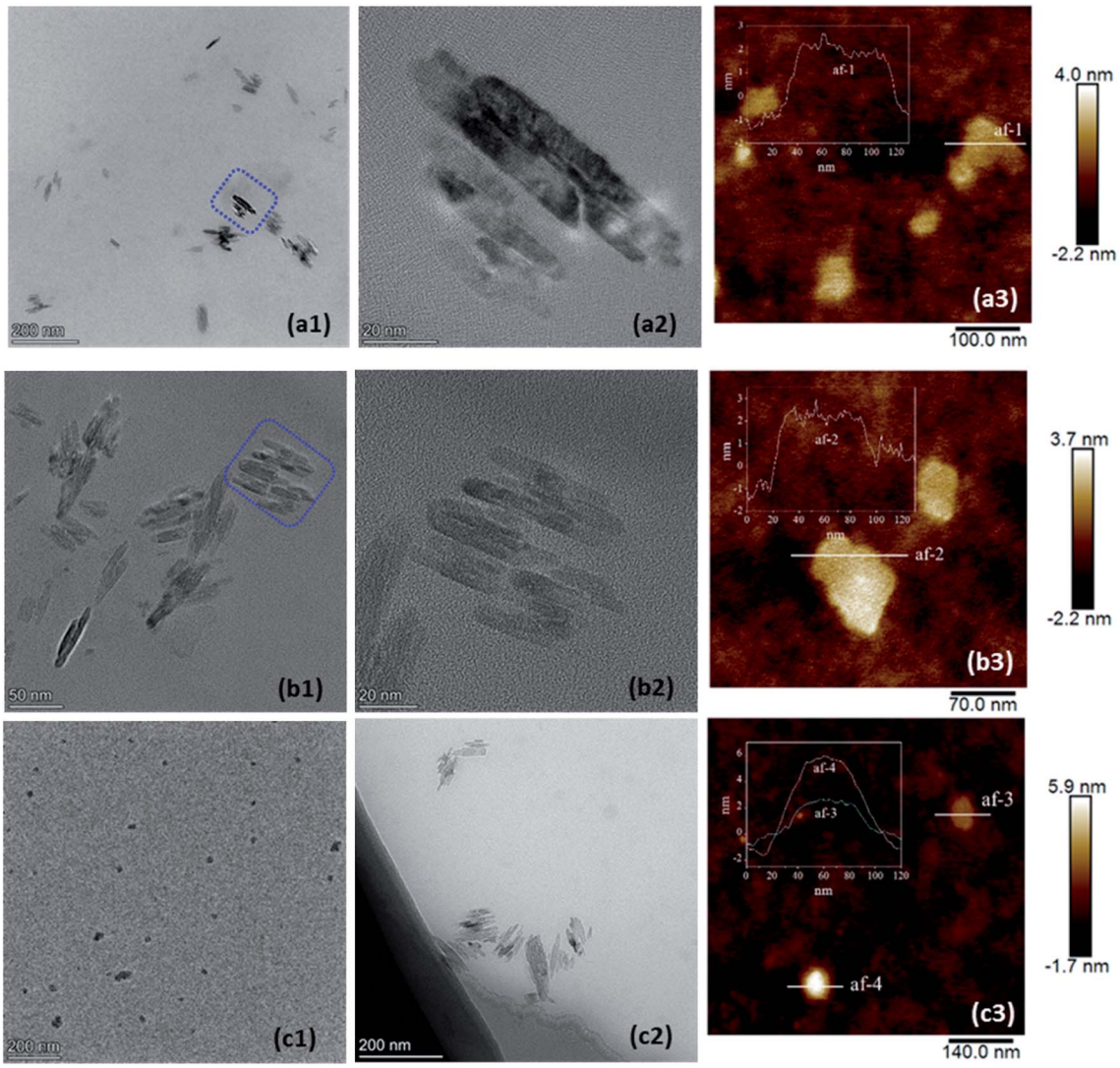

Fig. 2 TEM (a1, a2, b1, b2, c1 and c2) and AFM (a3, b3 and c3) images of the self-assembled aggregates from MSC23 (a1–a3), MSC33 (b1–b3) and MSC44 (c1–c3).

Open Access Article. Published on 06 March 2020. Downloaded on 2/14/2026 9:26:38 AM.
This article is licensed under a Creative Commons Attribution-NonCommercial 3.0 Unported Licence.

(or PEO-*b*-PDPA) were also investigated by other authors. For example, Yu and Li *et al.* obtained $mPEG_{114}$-*b*-PDPA wormlike micellar structure by a film sonication self-assembly method when mPEG weight fraction of $0.36 \leq W_{mPEG} \leq 0.48$.[40] Wu and Li *et al.* found that $mPEG_{44}$-*b*-$PDPA_{15}$ could form toruloid aggregates arranged by several single micelles at pH 7.4.[41] Xu and Kang *et al.* prepared $mPEG_{44}$-*b*-$PDPA_{80}$ spherical micelles in aqueous solution.[42] Mai *et al.* prepared PEO_{44}-*b*-PDPA micelles or polymersomes in water.[43] Some metallo-supramolecular block copolymers based on Tpy–metal coordination such as PS_{20}-[Ru(II)]-PEO_{70} (ref. 17) and PPG-[Cu(II)]-mPEG[22] self-assembled into spherical micellar morphology in water. PFS_{12}-[Ru(II)]-PEO_{70} (PFS, poly-(ferrocenylsilane))[20] formed cylindrical micelles in water. Therefore, our metallo-supramolecular complexes should exhibit different self-assembly fashion.

When mPEG(-*b*-Tpyp)$_2$-*b*-$PDPA_x$ are not coordinated by Ru(II) ions, the large and rigid Tpyp moiety only serves as a hydrophobic pendant group at the block junction point (Scheme 1e). Like some amphiphilic diblock copolymers, mPEG(-*b*-Tpyp)$_2$-*b*-$PDPA_x$ only self-assembled into spherical micelles in water (Fig. S8, ESI†), a very common and easily prepared morphology. But the formation of bis(terpyridine)-Ru(II) complexes made mPEG(-*b*-Tpyp)$_2$-*b*-$PDPA_x$ units orientational linkage *via* Ru(II) ions. Consequently, a positively charged rigid ···Tpyp-Ru(II)··· chain was created (Fig. 1A), because of rigidity of the Tpyp group itself and orientation of coordination bonding. Furthermore, the charge repulsion of ···Tpyp-Ru(II)··· chain may also enhance its rigidity. The mPEG/PDPA blocks thus changed into pendant chains of the complexes. Hence, the metallo-supramolecular complexes are polyelectrolytes with positively charged rigid chains along with the hexafluorophosphate (PF_6^-) counterions[11] and with a brush-like polymer architecture. When water induced self-assembly of the complexes, the aggregations of the rigid ···Tpyp-Ru(II)··· chains carrying the PF_6^- counterions and the hydrophobic PDPA blocks should be driving forces. Since the mPEG chains show a hydrated state and the PDPA blocks are not rigid in spite of their hydrophobicity, it is highly possible that the regular self-assembly of the metallo-supramolecular complexes was from directional arrangement of the rigid ···Tpyp-Ru(II)··· chains carrying the hydrophobic PF_6^- counterions. It was noted that MSC44 formed mixed spherical and sheet morphologies. This may be due to the fact that high DP of the PDPA block lowers the regularity of the supramolecular complex and enhances the intermolecular hydrophobic interaction, perturbing regular array of the rigid ···Tpyp-Ru(II)··· chains. It was also noted that the nanosheets from MSC33 were more stable than those from MSC23. Therefore, the PDPA block with an appropriate DP may be needed for metallo-supramolecular complex to self-assemble into a nanosheet morphology. According to the thickness of *ca.* 3.5 nm, it is speculated that the nanosheets should be a 2D monomolecular layer structure.[8] The self-assembly mechanism may be that the intermolecular aggregation of the rigid ···Tpyp-Ru(II)··· chains first formed a sheet, whose driving forces should be the hydrophobic and π–π interactions of the rigid chains. And the mPEG/PDPA pendant chains accordingly emanated from the two sides of the sheet. The mPEG chains showed an extended

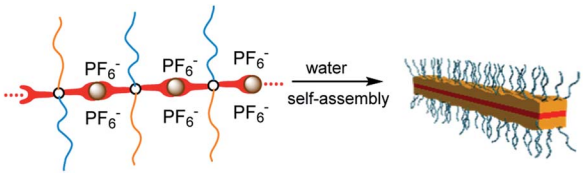

Scheme 2 A proposed pattern for self-assembled strip nanosheets.

state, guaranteeing water-solubility of the self-assemblies, while the PDPA blocks gradually formed inward collapsed hydrophobic domains and stabilized the nanosheets. A proposed self-assembly pattern for the nanosheets is shown in Scheme 2.

Owing to pH-sensitivity of the PDPA block (pK_a of protonated DPA homopolymer, ~6),[44] The influence of change in environmental pH on the morphologies of the self-assemblies above was also investigated by TEM observation. When the pH adjusted to 8.5, the morphologies of the self-assemblies didn't change evidently (Fig. S9a, S10a and S11a, ESI†) compared with those of their parent samples. Interestingly, when the pH of the solutions adjusted to 3.2, most of the strip nanosheet morphologies were destroyed due to the PDPA blocks changing into hydrophilicity, but nanosized aggregates were still observed from the three samples (Fig. S9b, S10b and S11b, ESI†). Wu and Li *et al.* reported that $mPEG_{44}$-*b*-$PDPA_{15}$ could not form apparent nanostructure at pH 5.5.[41] The observable aggregates of our samples should be attributed to the hydrophobic aggregation of the ···Tpyp-Ru(II)··· chains. Therefore, the hydrophobic interactions for the self-assembly of the complexes were from both the rigid ···Tpyp-Ru(II)··· chains and the PDPA blocks. And the formation and stability of the strip nanosheets were closely related to the hydrophobic interaction of the PDPA blocks.

The hydrophobic domains of the self-assemblies of the metallo-supramolecular complexes were further detected by fluorescence probe Nile Red (NR) (ESI†), because NR is fluorescent in hydrophobic environment but weak one in polar condition.[38,45] Herein the NR dosage used should not lead to visible precipitate when the THF was removed from the systems for self-assembly. The NR-loaded samples were diluted with water to 10 times for fluorescent spectrum measurement (Fig. S12, ESI†). The results indicate that samples NR/MSC44 (1.75/100, weight ratio), NR/MSC33 (0.75/100) and NR/MSC23 (1/100) showed fluorescent emission peaks at $\lambda_{em,\ max}$ = 571–574 nm (Fig. S12, ESI†).[38] Judged from the fluorescence intensity, a higher PDPA content formed a stronger hydrophobic domain in the aggregates (Fig. S12, ESI†). The TEM observations show that NR/MSC23 (1/100) self-assembled into mixed spherical micellar and nanosheet morphologies (Fig. S13a, ESI†) and NR/MSC44 (1.75/100) produced spherical micelles containing a small number of strip nanosheets (Fig. S13c, ESI†); while NR/MSC33 (0.75/100) mainly formed strip nanosheets (Fig. S13b, ESI†). It was found that the fluorescent intensities of the NR-loaded samples at $\lambda_{em,\ max}$ remained 75–80% after the incubation at 37 °C for 19.5 h. Then, the pH of the solutions was adjusted to 3.2, their fluorescent intensity lowered to 4–7% of initial values when measured after 30 min. This indicates that the NR molecules were initially mainly encapsulated in the

 This journal is © The Royal Society of Chemistry 2020

Open Access Article. Published on 06 March 2020. Downloaded on 2/14/2026 9:26:38 AM.
This article is licensed under a Creative Commons Attribution-NonCommercial 3.0 Unported Licence.

hydrophobic PDPA domains and the NR in the domains was therefore quickly released into polar water medium when the PDPA blocks changing into hydrophilicity at pH 3.2.

3. Conclusion

In summary, mPEG(-*b*-Tpyp)$_2$-*b*-PDPA$_x$ ($x = 23$, 33 and 44) block copolymer units were synthesized. After a hierarchical pattern of the coordination of the copolymers with Ru(II) ions followed by the self-assembly in water, strip nanosheets were obtained. And the parallel stripes along the length direction of the nanosheets were observed. Estimated from the thickness of *ca.* 3.5 nm for the nanosheets, they should be a 2D monomolecular layer structure. In contrast, mPEG(-*b*-Tpyp)$_2$-*b*-PDPA$_x$ without coordination formed spherical micelles. The formation of the strip nanosheets should be closely related to the architecture of the metallo-supramolecular complexes, *i.e.* the formation of the rigid ⋯Tpyp-Ru(II)⋯ chains, the PDPA block with an appropriate DP and its hydrophobic interaction, even the presence of the PF_6^- counterions. It is expected that the hierarchical self-assembly pattern can provide a new strategy of preparation of self-assemblies with different morphologies.

Conflicts of interest

The authors declare no conflict of interest.

Acknowledgements

This work was supported by the National Natural Science Foundation of China (No. 21871222).

Notes and references

1 H. Qiu, Z. M. Hudson, M. A. Winnik and I. Manners, *Science*, 2015, **347**, 1329–1332.
2 G. Rizis, T. G. M. van de Ven and A. Eisenberg, *Angew. Chem., Int. Ed.*, 2014, **53**, 9000–9003.
3 L. Cheng, G. Zhang, L. Zhu, D. Chen and M. Jiang, *Angew. Chem., Int. Ed.*, 2008, **47**, 10171–10174.
4 F. Xu, D. Wu, Y. Huang, H. Wei, Y. Gao, X. Feng, D. Yan and Y. Mai, *ACS Macro Lett.*, 2017, **6**, 426–430.
5 P. Zhou, Y.-Y. Liu, L.-Y. Niu and J. Zhu, *Polym. Chem.*, 2015, **6**, 2934–2944.
6 L. Niu, Y. Liu, Y. Hou, W. Song and Y. Wang, *Polym. Chem.*, 2016, **7**, 3406–3415.
7 Y. Hirai, T. Terashima, M. Takenaka and M. Sawamoto, *Macromolecules*, 2016, **49**, 5084–5091.
8 Y. Wei, J. Tian, Z. Zhang, C. Zhu, J. Sun and Z. Li, *Macromolecules*, 2019, **52**, 1546–1556.
9 J. Zhang, J. Liu, Y. Zhu, Z. Xu, J. Xu, T. Wang, H. Yu and W. Zhang, *Chem. Commun.*, 2016, **52**, 12044–12047.
10 Z. Wang, J. Gao, V. Ustach, C. Li, S. Sun, S. Hu and R. Faller, *Langmuir*, 2017, **33**, 7288–7297.
11 S. Kelch and M. Rehahn, *Macromolecules*, 1999, **32**, 5818–5828.
12 H. Hofmeier, S. Schmatloch, D. Wouters and U. S. Schubert, *Macromol. Chem. Phys.*, 2003, **204**, 2197–2203.
13 L. He, J. Liang, Y. Cong, X. Chen and W. Bu, *Chem. Commun.*, 2014, **50**, 10841–10844.
14 B. G. G. Lohmeijer and U. S. Schubert, *Macromol. Chem. Phys.*, 2003, **204**, 1072–1078.
15 H. Hofmeier, R. Hoogenboom, M. E. L. Wouters and U. S. Schubert, *J. Am. Chem. Soc.*, 2005, **127**, 2913–2921.
16 B. G. G. Lohmeijer and U. S. Schubert, *Angew. Chem., Int. Ed.*, 2002, **41**, 3825–3829.
17 J.-F. Gohy, B. G. G. Lohmeijer and U. S. Schubert, *Macromolecules*, 2002, **35**, 4560–4563.
18 J.-F. Gohy, B. G. G. Lohmeijer, S. K. Varshney, B. Décamps, E. Leroy, S. Boileau and U. S. Schubert, *Macromolecules*, 2002, **35**, 9748–9755.
19 M. Chiper, M. A. R. Meier, D. Wouters, S. Hoeppener, C.-A. Fustin, J.-F. Gohy and U. S. Schubert, *Macromolecules*, 2008, **41**, 2771–2777.
20 J.-F. Gohy, B. G. G. Lohmeijer, A. Alexeev, X.-S. Wang, I. Manners, M. A. Winnik and U. S. Schubert, *Chem.–Eur. J.*, 2004, **10**, 4315–4323.
21 C. Ott, R. Hoogenboom, S. Hoeppener, D. Wouters, J.-F. Gohy and U. S. Schubert, *Soft Matter*, 2009, **5**, 84–91.
22 B. Liang, R. Tong, Z. Wang, S. Guo and H. Xia, *Langmuir*, 2014, **30**, 9524–9532.
23 J.-F. Gohy, M. Chiper, P. Guillet, C.-A. Fustin, S. Hoeppener, A. Winter, R. Hoogenboomb and U. S. Schubert, *Soft Matter*, 2009, **5**, 2954–2961.
24 N. Hosono, M. Gochomori, R. Matsuda, H. Sato and S. Kitagawa, *J. Am. Chem. Soc.*, 2016, **138**, 6525–6531.
25 W. Zheng, L.-J. Chen, G. Yang, B. Sun, X. Wang, B. Jiang, G.-Q. Yin, L. Zhang, X. Li, M. Liu, G. Chen and H.-B. Yang, *J. Am. Chem. Soc.*, 2016, **138**, 4927–4937.
26 C. Kim and H. Kim, *J. Organomet. Chem.*, 2003, **673**, 77–83.
27 X. Yan, S. Li, T. R. Cook, X. Ji, Y. Yao, J. B. Pollock, Y. Shi, G. Yu, J. Li, F. Huang and P. J. Stang, *J. Am. Chem. Soc.*, 2013, **135**, 14036–14039.
28 Q. Zheng, Z. Ma and S. Gong, *J. Mater. Chem. A*, 2016, **4**, 3324–3334.
29 A. Winter and U. S. Schubert, *Chem. Soc. Rev.*, 2016, **45**, 5311–5357.
30 Y.-J. He, T.-H. Tu, M.-K. Su, C.-W. Yang, K. V. Kong and Y.-T. Chan, *J. Am. Chem. Soc.*, 2017, **139**, 4218–4224.
31 Y. Yan and J. Huang, *Coord. Chem. Rev.*, 2010, **254**, 1072–1080.
32 R. Shunmugam, G. J. Gabriel, K. A. Aamer and G. N. Tew, *Macromol. Rapid Commun.*, 2010, **31**, 784–793.
33 G. Gröger, W. Meyer-Zaika, C. Böttcher, F. Gröhn, C. Ruthard and C. Schmuck, *J. Am. Chem. Soc.*, 2011, **133**, 8961–8971.
34 X. Lu, X. Li, K. Guo, T.-Z. Xie, C. N. Moorefield, C. Wesdemiotis and G. R. Newkome, *J. Am. Chem. Soc.*, 2014, **136**, 18149–18155.
35 A. B. Padias and H. K. Hall, Jr, *Macromolecules*, 1982, **15**, 217–223.
36 B. Treetharnmathurot, C. Ovartlarnporn, J. Wungsintaweekul, R. Duncan and R. Wiwattanapatapee, *Int. J. Pharm.*, 2008, **357**, 252–259.

Open Access Article. Published on 06 March 2020. Downloaded on 2/14/2026 9:26:38 AM.
This article is licensed under a Creative Commons Attribution-NonCommercial 3.0 Unported Licence.

37 B. Parrish and T. Emrick, *Macromolecules*, 2004, **37**, 5863–5865.
38 Y. Wang, Y. Liu, J. Liang and M. Zou, *RSC Adv.*, 2017, **7**, 11691–11700.
39 K. Dayananda, M. S. Kim, B. S. Kim and D. S. Lee, *Macromol. Res.*, 2007, **15**, 385–391.
40 H. Yu, Z. Xu, D. Wang, X. Chen, Z. Zhang, Q. Yin and Y. Li, *Polym. Chem.*, 2013, **4**, 5052–5055.
41 W. Wu, W. Wang, S. Li, J. Wang, Q. Zhang, X. Li, X. Luo and J. Li, *J. Polym. Res.*, 2014, **21**, 494.
42 Z. Xu, P. Xue, Y.-E. Gao, S. Liu, X. Shi, M. Hou and Y. Kang, *J. Colloid Interface Sci.*, 2017, **490**, 511–519.
43 B. T. Mai, M. Barthel, R. Marotta and T. Pellegrino, *Polymer*, 2019, **165**, 19–27.
44 V. Bütün, S. P. Armes and N. C. Billingham, *Polymer*, 2001, **42**, 5993–6008.
45 M. K. Gupta, J. R. Martin, T. A. Werfel, T. Shen, J. M. Page and C. L. Duvall, *J. Am. Chem. Soc.*, 2014, **136**, 14896–14902.

 This journal is © The Royal Society of Chemistry 2020